LUND UNIVERSITY

Department of Solid State Physics

Masters Programme in Nanoscience

Optical characterization of patterned nanowire arrays using solid immersion microscopy

Supervisor:

Dan HESSMAN

By:

Gioele MALABARBA

September 2013

Abstract

The nanowires technology has proved itself to be fairly promising in order to develop more efficient optoelectronic devices such as solar cells and LEDs. It becomes therefore interesting to be able to characterize nanowires samples with a high precision, so that the light emitted from each single nanowire can be detected and analyzed. The purpose of this thesis project was to test if solid immersion microscopy represents a valid tool in order to increase the resolution of optical microscopy enough to distinguish between single nanowires in arrays. A solid immersion lens was fabricated, and then it was tested on a number of different samples in order to characterize it and to compare the results with the ones obtained by standard optical microscopy. Solid immersion microscopy led generally to a higher resolution in case of white light images. Photoluminescence and electroluminescence measurements were also performed; even though the experimental realization of such measurements was somehow trickier, solid immersion microscopy provides room for further improvements in resolution.

Contents

1 Introduction **3**

2 Light emission phenomena **5**

2.1 Photoluminescence in semiconductors 5

2.2 Electroluminescence in semiconductors 5

3 Experimental implementation **7**

3.1 Solid immersion lens 7

3.1.1 Resolution 8

3.1.2 Collection efficiency 9

3.2 Making the SIL 9

3.3 Microscopy setup 11

4 Presentation of samples and measurements **14**

4.1 Deposited broken nanowires samples 14

4.2 Nanopyramids sample 15

4.3 Standing nanowires sample I 20

4.4 Standing nanowires sample II 22

4.5 Standing nanowires sample III 24

4.6 Nanowires LED sample 26

4.7 Qualitative conclusions 28

5 Results and resolution evaluation **30**

5.1 Experimental magnification factor 30

5.2 Theoretical model for resolution evaluation 30

5.3 Experimental resolution evaluation 35

6 Conclusions and outlook **43**

7 Acknowledgements **45**

References **46**

Popular Science **47**

1 Introduction

Over the last years, research has greatly focused on developing better optoelectronic devices that convert light into electrical power and vice versa (i.e. solar cells and LED devices, respectively) with higher efficiency. The research on such devices based on the nanowires technology could lead to promising outcomes [1] [2]. Hence, a need to do optical characterization of nanowires rises, and since it is a light signal that should be detected and analyzed, optical microscopy is needed. Other imaging techniques such as Scanning Electron Microscopy (SEM)can reach very high spatial resolution but cannot detect a light signal coming from a LED device for example. Nevertheless, optical microscopy has its own limitations which lie mainly in the relatively low resolution due to diffraction and in the low collection efficiency (in case the signal to investigate is not very strong). Therefore it is from this perspective interesting to explore the resolution limits of optical microscopy, and to make an attempt to enhance its resolution as much as possible. Ideally it should be possible, in a nanowires array, to detect the light coming from each distinct nanowire, and to analyze it spectrally. This would be of great interest for example to get insight about the quality of the growth process. To this end, it has been chosen to apply the solid immersion microscopy method, which was introduced by Mansfield and Kino [3] [4] about twenty years ago and is based on a Solid Immersion Lens (SIL) placed directly in contact with the sample one wants to characterize. This approach has been succesfully employed in photoluminescence measurements on nanostructures [5] [6]. The SIL is usually a hemisphere of glass or material with high refractive index, and it should provide a number of advantages: its geometry is particularly designed not to introduce any geometrical aberration on top of those already present in the optical system; moreover, the SIL prevents a great internal reflection due to the strong difference in refractive indexes between the sample and the air. This concept is depicted and better explained in section 3.1.2.

The objective of this thesis is therefore to test the SIL approach and find out if it can be employed for this purpose. It has been tested with white light, photoluminescence and electroluminescence. Spectra and panchromatic images have been acquired from several different samples with both solid immersion microscopy and regular optical microscopy. A subsequent comparison between the two techniques provides useful insights on how much

the SIL approach can improve resolution and hence be useful in the characterization of single nanowires in nanowires array. This introduction is followed by a brief summary of photoluminescence and electroluminescence phenomena. In the third chapter, the experimental procedure to fabricate the SIL will be explained together with the experimental setup used to take images of the samples. The principles that underlie the usage of a SIL will also be explained. In the fourth chapter, the different samples on which the SIL was tested will be introduced, and the resulting images will be shown. In the final chapter, these results will be commented and a description of how the resolution is influenced by the presence of the SIL will be given.

2 Light emission phenomena

Since photoluminescence (PL) and electroluminescence (EL) signals were investigated during the thesis work, it is worthwile to have a brief explanation of the nature of both these phenomena. They are two particular kind of luminescence, which is the emission of light (not caused by heat) by a generic substance; the difference between them is of course the causes that determine the light emission. In the case of photoluminescence the light is generated subsequently to optical excitation (i.e. photons are absorbed into the sample) while in the case of electroluminescence the light is generated by electrons that are driven through a circuit. For further details, see [7].

2.1 Photoluminescence in semiconductors

In a semiconductor, a photon which possesses an energy larger than the bandgap energy can cause excitations of carriers with consequent formation of electrons in the conduction band and holes in the valence band with non zero momenta. Subsequently they undergo scattering and phonon interaction events as they reach the band gap minimum. If the material in question is a direct-gap semiconductor, then radiative recombination occurs when an electron-hole pair is close to the band gap minimum, and the wavelength of the emitted photon is correlated with the bandgap energy. A schematic illustration of a typical PL process is shown in figure 1. PL at room temperature usually results in a rather broad spectral emission, centered around the band gap minimum transition energy. In relation to figure 1 this can be explained with the fact that thermal energy causes electrons and holes to have higher momentum values and hence the transitions are more likely to occur even if the electrons have not reached the bottom of the band. This result obviously in emitted photons which have a higher energy than E_g, and a wavelength distribution which is broadened by thermal excitation.

2.2 Electroluminescence in semiconductors

Electroluminescence is a light emission process connected with an electrical excitation, which can be caused by the presence of a strong electrical field or an electrical current. In a semiconductor, electroluminescence occurs as a consequence of recombination between electrons in the conduction band and holes in the valence band. This happens for example in a direct biased p-n

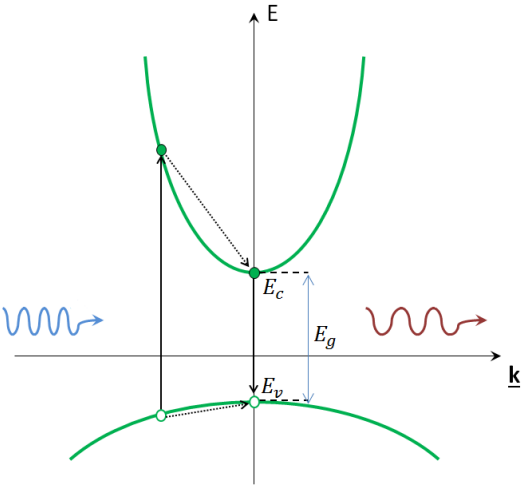

Figure 1: Schematic view of the PL process in a direct band gap semiconductor.

junction, which is the basis for a LED (Light Emitting Diode) device. The bias injects both electrons and holes in the junction, and light is emitted after radiative recombination. The wavelength of the emitted light depends on the semiconductor band gap. The basic functioning of a LED device is shown in figure 2.

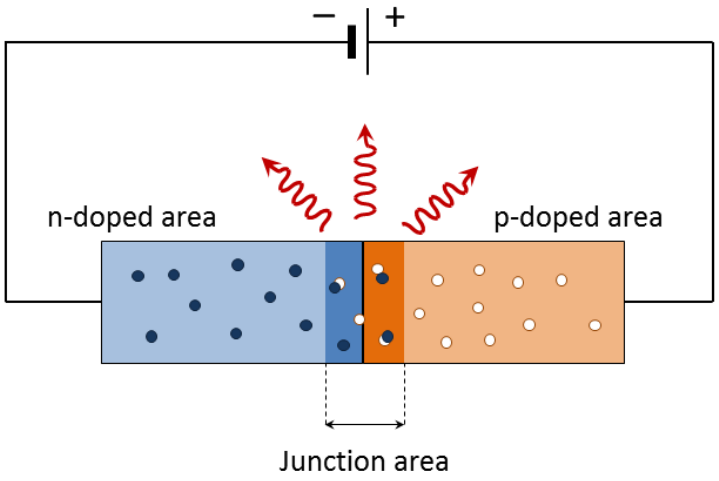

Figure 2: Schematic view of the EL process in a forward biased p-n junction.

3 Experimental implementation

3.1 Solid immersion lens

As the name suggests, the principles that underlie solid immersion microscopy are similar to the ones that underlie oil immersion microscopy. In the latter, both the objective and the object are immersed in an oily medium whose refractive index is higher than 1, which brings advantages in resolution [3] [8] and collection efficiency [9]. In the former, a special lens is designed to give the same result as if the object was immersed in a solid material. As far as this thesis is concerned, a half spherical SIL was used, as illustrated in figure 3.

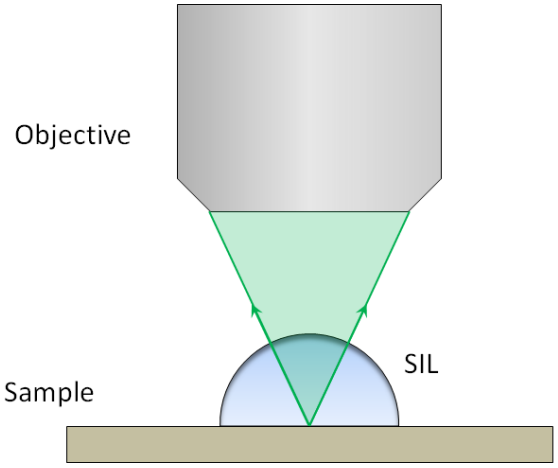

Figure 3: Schematic view of the SIL functioning. The green area represents the portion of the light emitted in correspondence of the center of the SIL which is collected by the objective.

As previously mentioned, the solid immersion lens lies in contact with the sample. In this way it is as if the object lied immersed in the solid material the lens is made of, since the light does not travel through any air when it is emitted from the sample, nor it meets a sample-air interface. The air is reached at the interface with the lens, but no internal reflection occurs since the light is travelling perpendicularly to the interface, and the geometry of the lens itself avoids geometrical aberrations.

3.1.1 Resolution

The spatial resolution of an optical system is defined as the ability of the system to distinguish between two point sources separated by a small distance. A higher resolution allows to distinguish between objects placed at smaller distances. Even for a perfect system, the size of the image is larger than the size of the object due to diffraction in the objective, and a point object will result in an image with an intensity distribution which follows the Airy function. The intensity profile of the Airy disk is shown in figure 4. The

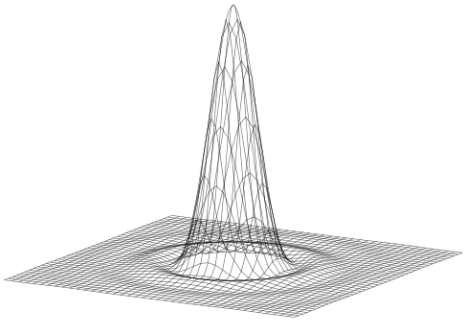

Figure 4: The Airy disk.[10]

Rayleigh criterion, invented by Lord Rayleigh, states that two point sources are considered to be resolved when the principal diffraction maximum of one image coincides with the first minimum of the other. This entails that the minimum distance between the sources that allows the system to resolve them is:

$$\Delta x = \frac{1.22\lambda}{2nsin\vartheta} \tag{1}$$

where λ is the wavelength of the light in vacuum and ϑ is half the collection angle. n is the refractive index of the medium between object and objective (in the case of optical microscopy, air). As it can be easily seen, a higher refraction index allows to resolve objects put closer to each other. For this reason, using a SIL with refractive index n will theoretically enhance the resolution by a factor n, as if the two objects were immersed in a solid medium.

3.1.2 Collection efficiency

The collection efficiency is particularly important in case the intensity of the signal is very weak and it is therefore necessary to collect and convey to the objective as much light as possible in order to have a better image. In the case of a hemispherical SIL there is no refraction at the surface between the SIL and the air, since the light propagates perpendicularly to it. The SIL has therefore the only effect to increase the numerical aperture of the system, which will be the numerical aperture of the objective multiplied by a factor n. The numerical aperture of an optical system is defined according to the following equation:

$$NA = nsin\vartheta, \tag{2}$$

where ϑ is half the angle of the maximum cone of light that is collected by the objective. The effect of the SIL will be to enhance the collection efficiency of the whole system [11].
Another issue that needs to be taken into account is the presence of an air gap between the sample and the SIL. The presence of such a gap would cause internal reflection at the sample-air surface (as shown in figure 5), and also a bad coupling of the evanescent wave in the SIL itself. Filling the air gap with a high refractive medium, that can be oil or wax for example, will solve this problem as it will lower the internal reflection in the sample and will improve the coupling of the evanescent signal in the SIL. As a result, the collection efficiency will be again improved.

3.2 Making the SIL

The SIL was fabricated manually, starting from a 3 mm diameter glass sphere made of LaSFN9, which is a fairly cheap material with refraction index that varies between 1.85 and 1.83 in the spectral region 600 nm - 900 nm [12]. The sphere was attached to a holder with some wax, and the holder was placed into a grinder in order to scrape the sphere with sandpaper. The grinder had a micrometer that allowed to control the thickness of the portion of the SIL that was being scraped. The goal was to make a perfect hemisphere out of a 3 mm diameter sphere, hence the total thickness that was to be grinded was 1500 μm. Most of the material was removed using a 1000 mesh sandpaper. The last few hundreds μm were removed using a 2500 mesh sandpaper instead. Finally, a negligible amount of material was

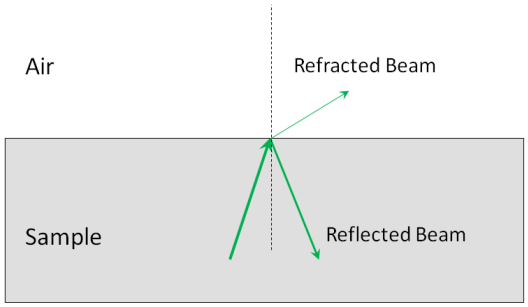

Figure 5: Schematic depiction of the internal reflection process. When a beam is travelling in the sample and it encounters an interface with air, part of the beam will be reflected back into the sample and part of the beam will pass through according to diffracion laws. The intensity of the reflected beam increases with the difference between the refractive indexes (sample and air in this case) and also with the incidence angle.

grinded during the polishing process, which was realized with a 4000 mesh sandpaper.

As described earlier, the SIL needs to be put in close contact with the sample, and a thin layer of material with a high refractive index is recommended between the SIL itself and the substrate; hence it was decided to use an oil for oil immersion microscopy, Immersol 518F from Zeiss [13], with a refractive index of 1.518 at room temperature. The SIL was cleansed with acetone and isopropanol and then rinsed with water before it was put on each sample. To put the SIL on a new sample, first an oil drop was placed onto the surface and then the SIL was gently placed over it, without applying any pressure. Using the oil allows the SIL to slide over the sample, which brings both advantages and disadvantages. The advantage is that in this way one can easily move the SIL and consequently change the part of the sample that is being looked at; this is useful since placing the SIL on the right spot is tricky, because of course it is a macroscopic object being placed where one wants to look at nano-features. On the other hand, this results in a lack of control over the position in which the SIL is put, which makes it really hard to look

at the exact same area on a sample in different measuring sessions. As an alternative to oil, wax could have been used. This would have provided more stability but it would have made it impossible to move the SIL once it had been placed on the sample.

3.3 Microscopy setup

The experimental setup used during the project work is shown in figure 6. The sample is mounted onto a 2D translation stage, and an optical micro-

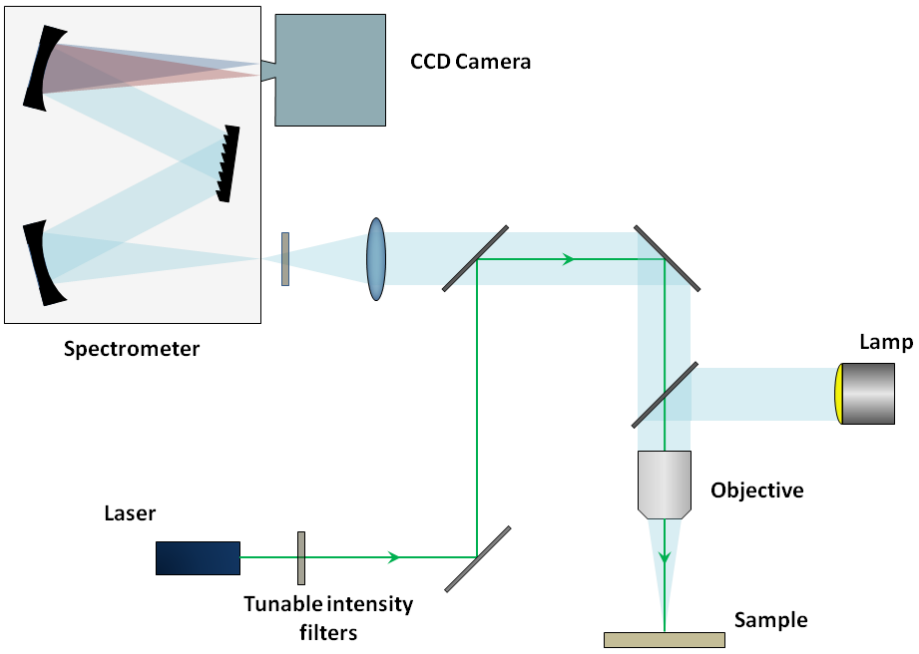

Figure 6: Schematic view of the experimental setup. The SIL, when used, is positioned on top of the sample, so that the laser beam hits the sample in correspondence to the center of the SIL.

scope with a 100x objective was used. A lamp (white light source) was used when taking panchromatic images and reference images, whereas a laser in continuous wave mode was used as an excitation source in PL measurements. A few different lasers were used throughout the project, depending on the wavelength needed for each sample:

- Green frequency doubled YAG laser, with 532 nm emission wavelength

and 125 mW full power output.

- UV semiconductor laser, with 375 nm emission wavelength and 495 mW full power output.
- UV He-Cd laser, with 325 nm emission wavelength and 200 mW full power output.

As it can be seen from figure 6, the excitation is performed through the objective, which means that the laser light is brought from the laser source to the sample through a system of lenses and mirrors so that the beam follows the same optical path that the PL signal follows while going out of the microscope to the spectrometer. This results in normal incidence of the laser beam onto the sample. This configuration has been chosen instead of the one in which the laser beam hits the sample from the side mainly because of two reasons. The first one is that the laser beam should hit the sample in correspondence to the center of the SIL, since the only "useful" area that one can look at with the SIL is a circle with the diameter of a few hundred micrometers. This can be better understood by looking at figure 7. Outside of this area the emitted light deviates from the ideal case depicted in

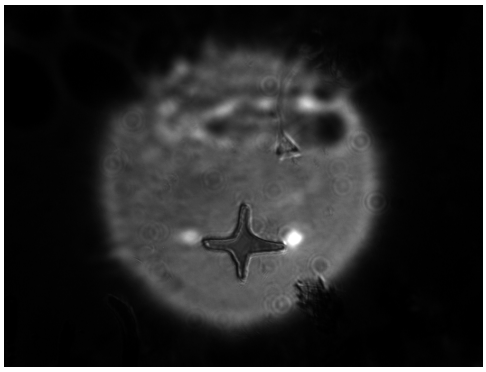

Figure 7: Optical image taken with the SIL and a 5x objective. The size of the cross is roughly 100 μm.

figure 3 and all the advantages of the SIL are rapidly lost as one gets further away from the centre (i.e. the light is refracted at the SIL-air interface and geometrical aberrations occur). With the laser beam coming from the side, it becomes obviously difficult to establish whether or not the beam hits the sample in correspondence to the center of the SIL, especially if the SIL itself has no fixed position and can slide over the sample. The second reason is

that if the SIL is hit from the side, the laser light undergoes many undesired reflections that cause losses, and in the worst case the power is not even enough to generate a PL signal. The white light used to take conventional images also comes from the same direction. The signal is then sent to the spectrometer, which is controlled by a computer and connected to a CCD camera. A lens is placed in front of the spectrometer in order to focus the signal through the slit. It was possible to take images both in mirror mode and in spectral mode. In mirror mode the spectrometer works as a mirror, so that all light within the detectable wavelength region is collected by the CCD. In spectral mode on the other hand the spectrometer is configured to reflect only a selected wavelength interval onto the CCD camera. 3D graphs of the intensity versus a spatial coordinate on one axis and a spectral coordinate on the second axis could also be taken, if one direction in the CCD camera was used to store spectral information instead of spatial information. Filters were set in the optical path of the laser when performing a PL measurement: a set of attenuation filters was placed right after the laser device, in order to adjust the output power to the desired level, and another filter was placed in front of the spectrometer, in order to filter all the laser light and detect only the PL signal.

4 Presentation of samples and measurements

Once the SIL was fabricated, a number of different samples were used in order to characterize it and in order to evaluate how much it could improve the resolution. In this section, all the samples will be introduced with their properties, along with images taken with and without the SIL. The comparison between the images will give a general idea about how the presence of the SIL affects the measurements, whereas a more quantitative analysis is left for the next chapter.

4.1 Deposited broken nanowires samples

The first samples to be investigated consisted of silicon substrates with a gold-patterned surface. The presence of a pattern allowed to estimate the magnification factor introduced by the SIL in the system. Note that the theoretical magnification factor introduced by the SIL itself has been shown to be equal to the refractive index n of the material of which the SIL is composed [3]; measuring on these samples allowed to get an experimental evaluation of the magnification introduced by the combination of SIL and immersion oil used to fill the gap between the SIL and the sample.
In addition to this, nanowires of two different dimensions were scraped off from as-grown samples and deposited onto the gold patterned silicon samples. Width and length of the nanowires are listed in table 1.

Table 1

	Length	Width
Sample 1	4 μm	80 nm
Sample 2	5 μm	130 nm

The purpose of the presence of these deposited nanowires was to get an idea of how small objects could be actually be detected using solid immersion microscopy, and also to characterize the resolution of the system. More details are provided in chapter 5. Images from the samples were taken both without the SIL (i.e. with normal optical microscopy) and with the SIL. The comparison between the two images provides useful information on how the presence of the SIL improves the quality of the measurement. This approach has been used throughout all the experimental work, with all samples. Im-

ages taken from Sample 2 are shown in figure 8. The contrast is comparable

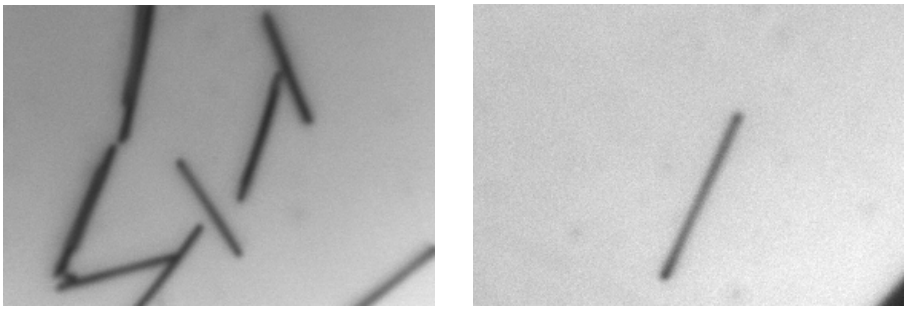

(a) Image taken without the SIL. (b) Image taken with the SIL.

Figure 8: Broken nanowires deposited on sample 2.

in the two pictures, and so seems to be also the thickness of the nanowires. This would suggest that there is an actual improvement in the resolution: if the resolution was the same, then the thickness of the nanowires should appear increased by the magnification factor introduced by the SIL. How the resolution is actually affected will be evaluated in the following chapter. The magnification introduced by the SIL was calculated from the comparison between the size of pattern features in the sample. Comparing the size of the same feature (in terms of pixels) in pictures taken both with and without SIL, allowed to give an experimental estimate of the magnification factor of the SIL. For this purpose it was not necessary to know the actual dimensions of the feature, since it was only the relative magnification that mattered.

4.2 Nanopyramids sample

The first sample to be investigated, once that the magnification introduced by the SIL was estimated, was composed by a hexagonal pattern of gallium nitride pyramids. An image of the sample acquired with the SEM is shown in figure 9. The distance between the tops of the pyramids is 1 μm, and their width resulted to be approximately 600 nm. In figure 10 images of the same sample taken with optical microscopy and with solid immersion microscopy are shown. These two images were taken in order to compare the resolution in the two different microscopy modes. As a matter of fact, the focusing lens in front of the spectrometer was placed 200 mm far from it in the measurement without the SIL, and 100 mm far from it in the measurement with the SIL. The distance of the focusing lens from the spectrometer influenced the

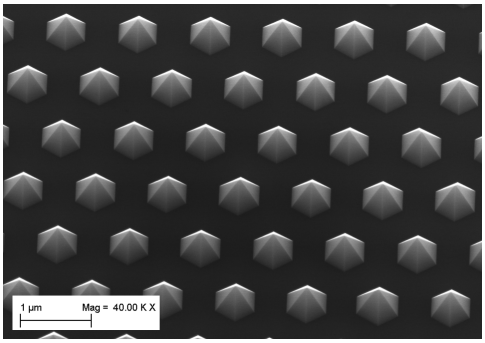

Figure 9: SEM image of the pyramids sample.

magnification of the images. For this reason, the total magnification of the two images is roughly the same, since the magnification introduced by the SIL is compensated by an increased distance of the focusing lens. Thus, the two images can be better compared in order to evaluate the resolution. As

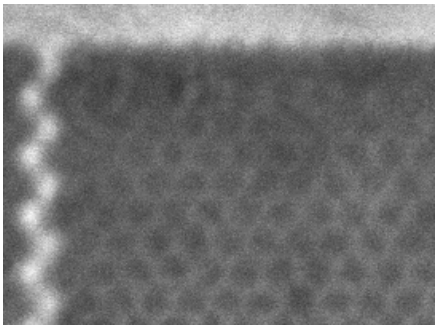

(a) Image taken without the SIL.

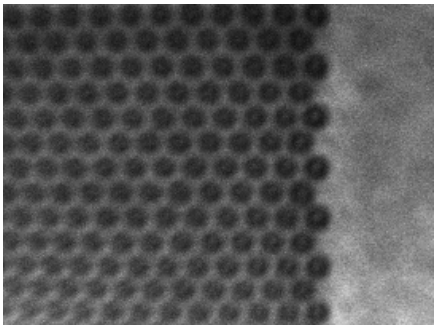

(b) Image taken with the SIL.

Figure 10: White light images from the pyramids sample.

it can be easily seen from figure 10, a good contrast was achieved with the SIL, while it seems more difficult to distinguish between the single pyramids in the image without the SIL.

PL measurements were also performed on this sample. The pyramids were expected to have a PL peak around 450 nm, hence the Helium-Cadmium UV laser with emission wavelength 325 nm was used. Two images taken with the SIL in the same spot but under different focusing conditions are presented in figure 11. The fact that it was possible to obtain images of the pyramids both as bright and dark dots suggested that the signal detected could actually be a reflection of the laser light that went through the spectrometer despite the

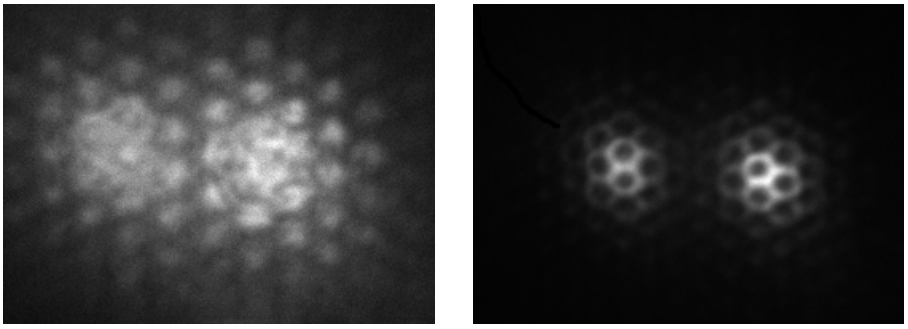

(a) (b)

Figure 11: PL Images from the pyramids sample, under different focusing conditions.

presence of a filter. This led naturally to the next step of the work, which was to take spectral PL measurements. Since the PL emission spectrum of the pyramids (and more in general, of all the samples inspected with the SIL) was known, taking spectral measurements allowed to get a better insight about where the detected light was emitted, and how much of it actually came from the pyramids. To this purpose, spectra of the light emitted by the sample were recorded in two different spots, one where there were actually pyramids (under focus conditions as in figure 11a), and the other where there was just bare substrate. The spectra are shown in fig 12. The spectrum measured on the substrate shows rather sharp peaks, but nevertheless no PL peak around 450 nm, which is instead shown by the spectrum in figure 12b. This suggests that part of the light measured in figure 11a is actually generated by PL in the pyramids. On the other hand, the intensity of the PL peak is much lower compared to the intensity of the other peaks; even if these peaks appear to be broader in figure 12b than in figure 12a, it is still unlikely that they could be due to PL. The origin of these peaks is uncertain. In figure 13 two line by line spectra are shown, both taken from the pyramids but under different focusing conditions, similarly to what was shown in figure 11 (i.e. figure 13a refers to a focusing condition that makes the pyramids appear as bright spots, and figure 13b to a condition in which they appear as dark spots). It is easily seen that the PL feature around 450 nm is absent in figure 13b, while it appears in figure 13a. This means that when the pyramids appear as dark spots, the light that is being detected actually comes only from the substrate, not from the pyramids. On the other hand, when they appear as

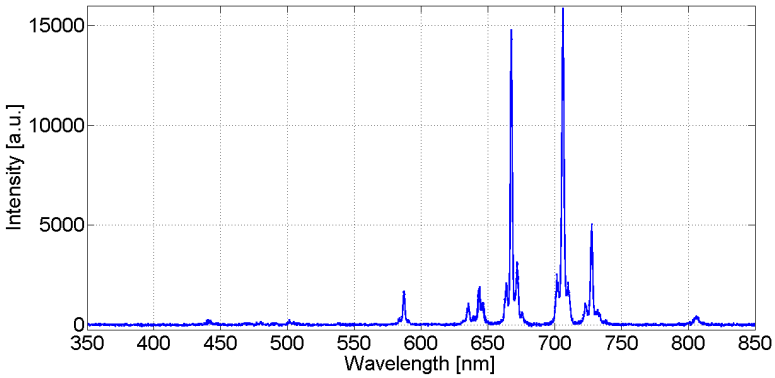

(a) Spectrum of light emitted from the substrate.

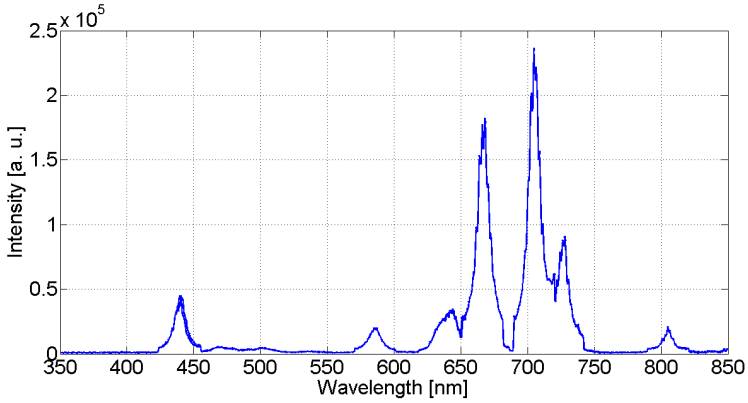

(b) Spectrum of light emitted from the pyramids.

Figure 12: Spectral PL measurements on the pyramids sample, using the SIL.

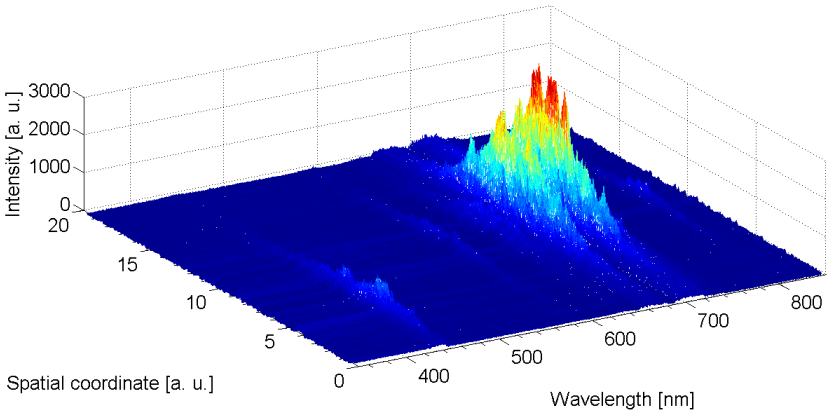

(a)

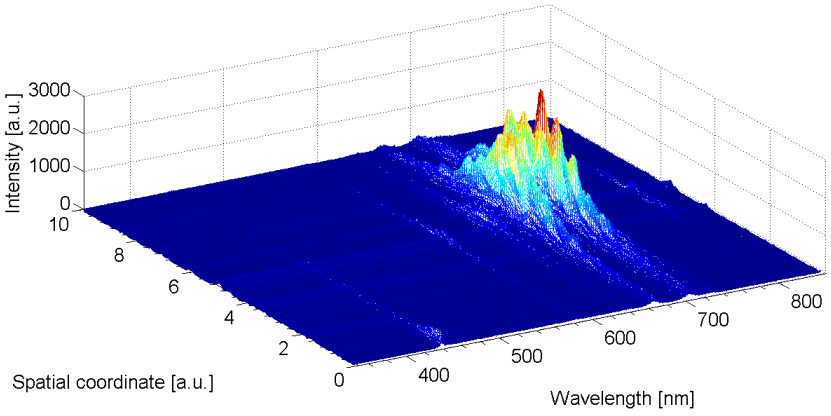

(b)

Figure 13: Line by line spectral PL images of the pyramids sample.

bright spots, most of the light still comes from the substrate, but there is also a PL contribution from the pyramids. It becomes evident though that the light around 450 nm do not allow to distinguish between pyramids. On top of this, considerable absorption of the laser light at 325 nm occurred both in the SIL and in the objective lens. For this reason the PL peak was also much weaker than the other reflection peaks.
All in all, this sample proved itself to be not so interesting to inspect as far as PL is concerned, also because the dimensions involved were rather big compared to the ones displayed by nanowires arrays. Nevertheless, it allowed to test and characterize better the SIL itself and showed that the SIL might have the potential to improve the resolution of optical microscopy.

4.3 Standing nanowires sample I

This sample was chosen because of the good photoluminescence emission, with an expected peak around 860 nm at room temperature. The green laser (output wavelength 532 nm) was used as the excitation source. It consisted of a $GaAs$ substrate on which nanowires had been grown with a honeycomb pattern with 1 μm pitch. The nanowires had a core-shell structure with a $GaAs$ core and a $AlGaAs$ shell, for a total thickness between 160 nm and 180 nm. The total length of the nanowires was around 2,4 μm. A picture of the sample, taken with the SEM, is shown in figure 14. One

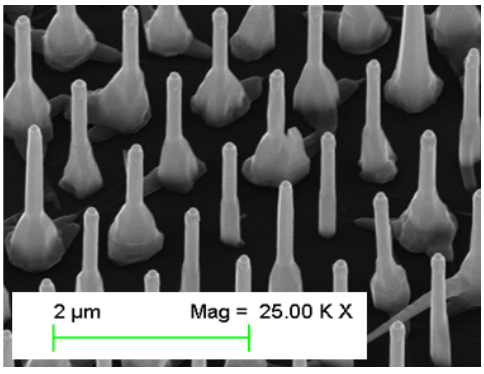

Figure 14: SEM image of Sample I.

can easily notice the presence of some parasitic growth on the base of the wires. Optical microscopy images from the sample are shown in figure 15, both with and without using the SIL. The contrast seems once again to be roughly the same with and without the SIL, but the image taken with solid

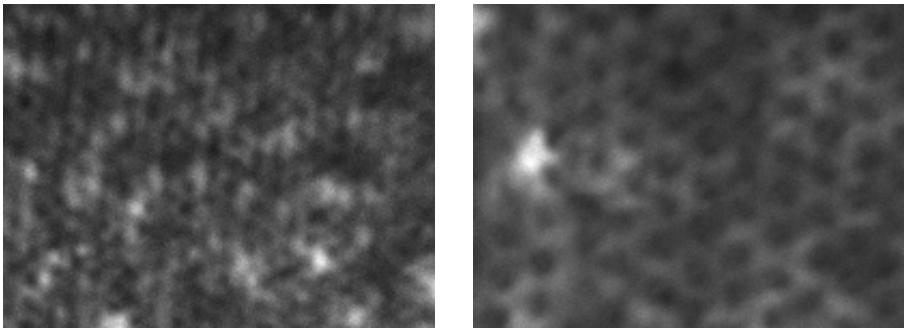

(a) Image taken without the SIL. (b) Image taken with the SIL.

Figure 15: Optical images of Sample I.

immersion microscopy displays a higher magnification, which might suggest an improvement in resolution. There seems to be also a very non-uniform background signal; this could be due to the parasitic growth on the base of the wires, that reflected the reference light differently in every spot.
In figure 16 the results from PL measurements on the sample are shown. In

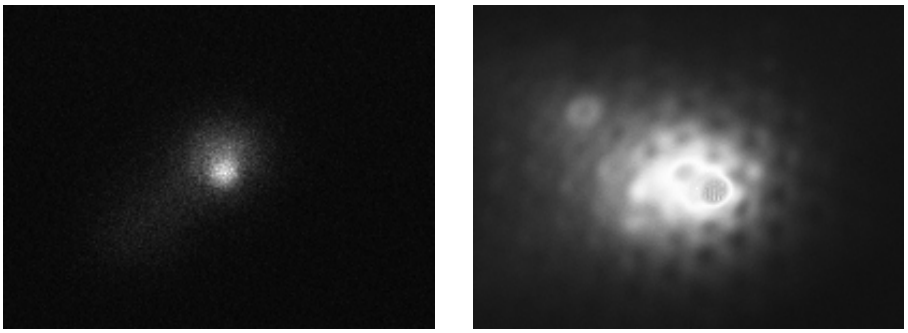

(a) PL Image taken without the SIL. (b) PL Image taken with the SIL.

Figure 16: PL images of Sample I.

this case the improvement brought by the SIL is evident, as the nanowires could not be distinguished with normal optical microscopy, while solid immersion microscopy allowed to see single nanowires. In spite of that, the same phenomenon that occurred with the pyramids sample can be observed: the nanowires appear actually as dark dots whereas they should appear as bright dots, since they are emitting light. In this case however, this is due to the fact that the substrate is also emitting PL signal, at the same wavelength expected for the nanowires (the nanowires and the substrate are actually

made of the same material, so they both generate a PL signal at the same wavelength). This can be seen from the inspection of a line by line spectrum, shown in figure 17. Here one can see just one broad peak, at around 860 nm. It was possible to distinguish the presence of single nanowires on this

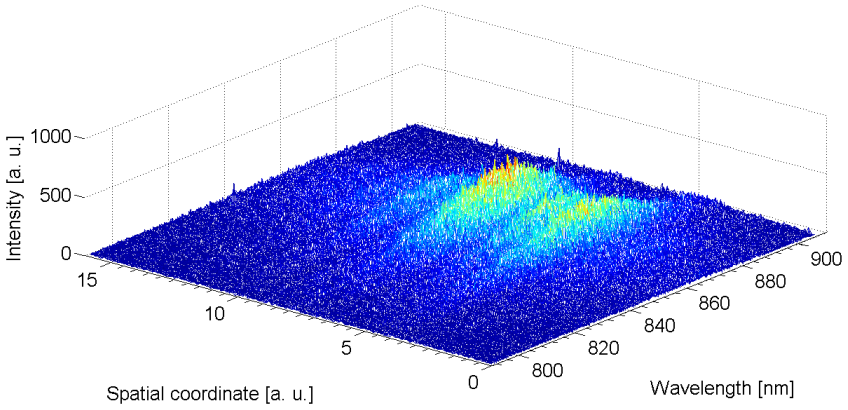

Figure 17: Line by line PL spectrum of Sample I.

sample, but not to detect the light coming from distinct nanowires, because of the emitting substrate. It was hence necessary to look for nanowire samples whose substrate material would be different than the one the nanowires were made of, so that the PL signal could be emitted only by the nanowires, or at least a sample where the nanowires had a stronger emission intensity compared to the substrate (e.g. by absorbing most part of the incoming laser light, so that excitation in the substrate would not occur).

4.4 Standing nanowires sample II

This sample should have provided a good PL behaviour, in the sense that the nanowires were supposed to absorb most of the light that hit the sample. The sample consisted in standing InP nanowires with a diameter of about 130 nm, disposed in rows with a pitch of 400 nm. The substrate material is InP as well. The green laser with emission wavelength 532 nm was used in PL measurements. In figure 18 two different EM images can be seen, one from the top (figure 18a) and one close-up from the side (figure 18b). In figure 19 two white light images, taken with and without the SIL, are shown. It becomes evident from the comparison of the two images that in such sample the introduction of the SIL allowed to get a better magnification of the

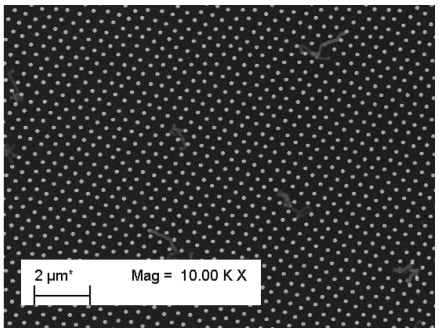

(a) SEM image, top view.

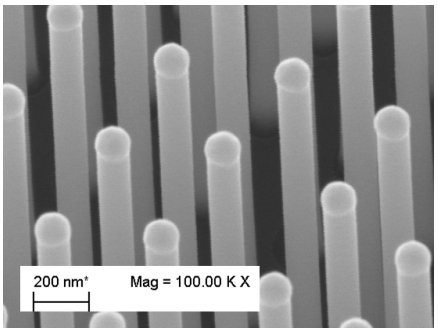

(b) SEM image, side close-up.

Figure 18: SEM images of Sample I.

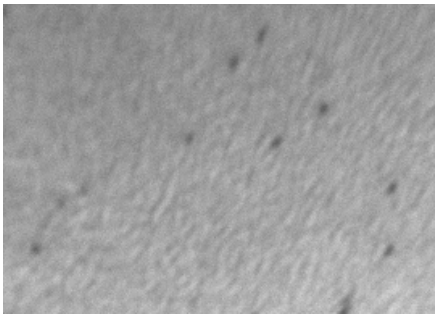

(a) Image taken without the SIL.

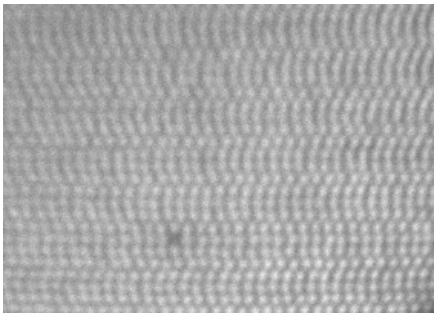

(b) Image taken with the SIL.

Figure 19: Optical images of Sample I.

sample, as well as a better contrast. This suggests that the solid immersion technique can be promising in order to enhance the resolution as well. As far as PL is concerned, the SIL also allowed to distinguish between single nanowires, as figure 20 shows, whereas it was impossible with normal optical microscopy. The PL wavelength was actually the expected one, wihtout any contribution from the substrate or other phenomena altering the spectrum. The excitation area was quite small, hence only a few nanowires emitted

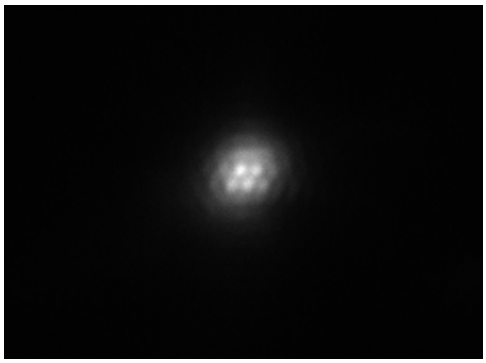

Figure 20: PL image of Sample II, taken with the SIL.

enough light to be detected. A broader laser spot would have allowed to resolve well the single nanowires over a bigger area in the sample.

4.5 Standing nanowires sample III

This sample was rather similar to the sample discussed in section 4.4; it consisted of InP nanowires with a wurtzite structure, grown on a substrate with a zincblende structure. In this case the different cristal structures in the nanowires and the substrate caused the emission energies to be different, which allowed to separate the signal coming from the nanowires and the signal coming from the substrate at some extent. The pitch between the nanowires was 500 nm. In PL measurements, the green laser ($532nm$) was used as excitation source. A SEM image of the sample is shown in figure 21. In figure 22, images taken respectively with optical microscopy and solid immersion microscopy are shown. Once again, the introduction of the SIL allows to see a better distinction between the nanowires in the array. In figure 22a the presence of the nanowires can be seen, but they would probably not be resolved according to Rayleigh criterion. In figure 22b on the other hand, the nanowires can be resolved quite clearly with white light microscopy. PL

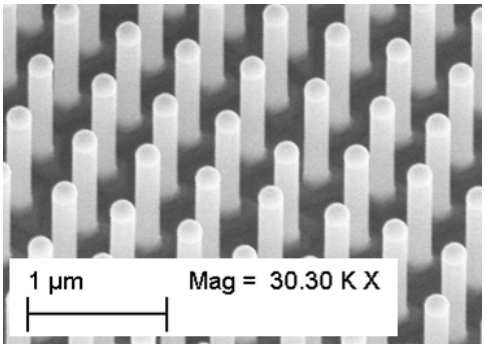

Figure 21: SEM image of Sample III.

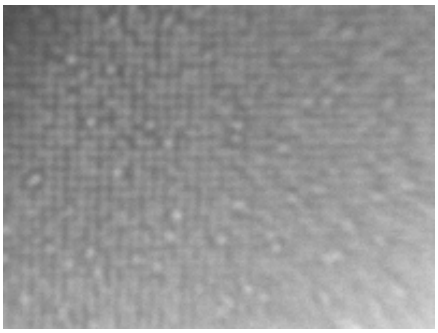

(a) Image taken without the SIL.

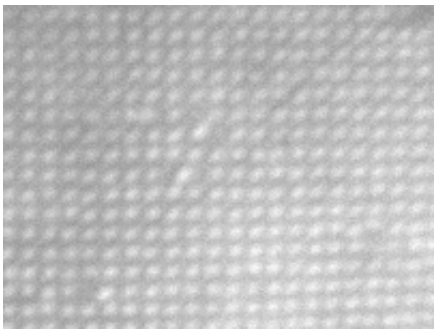

(b) Image taken with the SIL.

Figure 22: Optical images of Sample III.

measurements were also performed on the sample, with the results presented in figure 23. In PL measurements, the nanowires cannot be distinguished

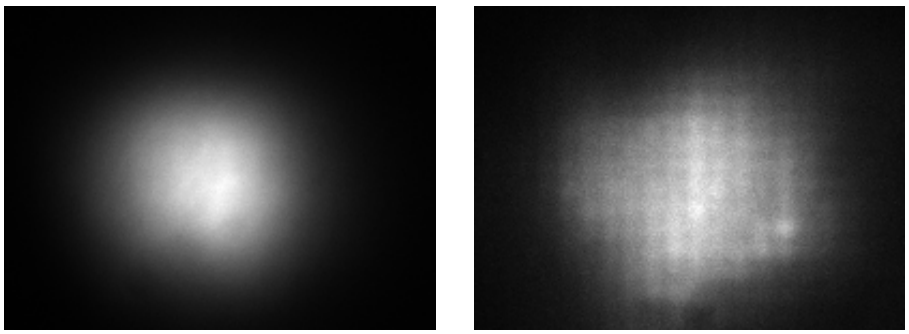

(a) PL Image taken without the SIL. (b) PL Image taken with the SIL.

Figure 23: PL images of Sample III.

without the SIL. Their presence can be seen with the SIL instead, but they are probably not resolved.

4.6 Nanowires LED sample

The last sample which was investigated was a nanowire based LED. The nanowires were standing in a hexagonal pattern with 2,5 μm pitch. The measurements on this sample were performed with a slightly different implementation, since the bond contacts prevented the SIL to be placed in direct contact with the sample; hence, a different SIL with thickness 1,4 mm was used. This difference was compensated by keeping the SIL at a distance of 100 nm from the sample, which was enough to fit the contact wires connected to the sample. To this end, the SIL was mounted on a special separate stage which could be moved in three dimensions in order to vary the actual distance between sample and SIL and focus the image in a proper way. This way, the sample could be moved without moving the SIL and vice versa. The modified SIL set up is shown in figure 24. A reference light image was taken without the SIL, as shown in figure 25. The pitch was rather large, especially in comparison with the samples of section 4.4 and 4.5. Hence the nanowires are resolved already without using the SIL. Two images of the functioning device (EL measurements), are on the other hand shown in figure 26. In this case, in spite of the magnification factor, there is not an evidence to suggest that the SIL improves the resolution of the image. This could be due to the introduction of the separate stage for the

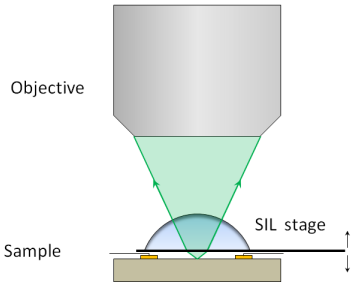

Figure 24: Schematic view of the SIL functioning for LED measurements.

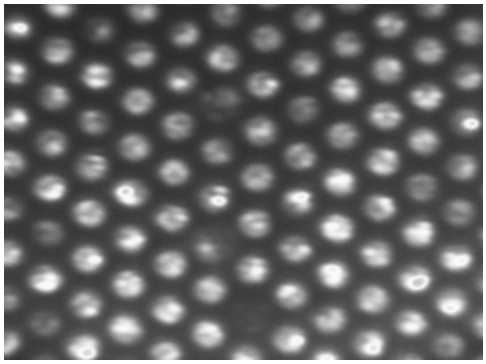

Figure 25: Image of the NW-LED sample, taken without SIL.

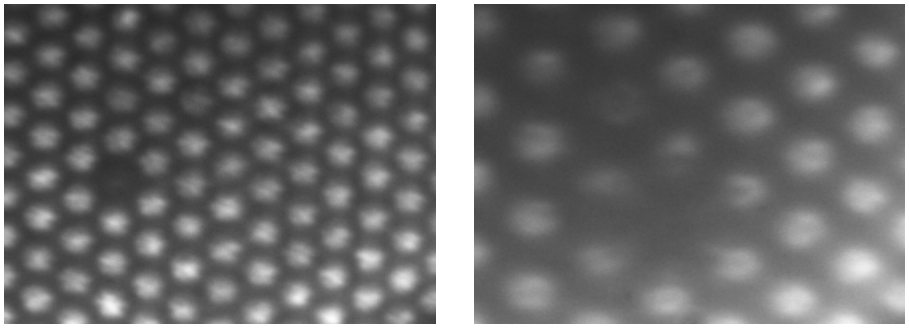

(a) EL Image taken without the SIL. (b) EL Image taken with the SIL.

Figure 26: EL images from the NW-LED sample.

SIL, that actually introduced more degrees of freedom in the measurement as well as tilt problems, making it harder to reach the optimal conditions. Nevertheless, imaging of single nanowires could be performed.

4.7 Qualitative conclusions

In conclusion, the SIL proved itself to be a valuable and promising addition to normal optical microscopy, if one wants to increase the resolution of the measurements. Especially as far as white light microscopy is concerned, the improvement introduced by the SIL is evident, and this comes as a clear result from the comparison between optical microscopy and solid immersion microscopy over different samples (see figures 10, 15, 19 and 22). In most cases images taken with the SIL show higher magnification as well as better contrast compared to the ones taken without the SIL. With PL measurements on the other hand, the SIL seems to introduce anyway an improvement, but the extent of this improvement might actually depend from the sample itself. In some cases the signal coming from the nanowires might not be detected at all, if the substrate itself emits, as in the case of Sample I. The quality of the sample also plays a role, defects like parasitic growth lower the quality of the measurements and consequently the resolution. Sample II proved itself to be fairly good at this purpose. The white light image taken with the SIL allowed to distinguish the nanowires very well, and also in the PL image they seemed to be well resolved. To this purpose, it is useful to compare it with Sample III in order to get better insight on how sample features influence the quality of the images. Sample III had a slightly bigger pitch (500 nm, vs. 400 nm), so in principle it should be easier to distinguish individual nanowires than in Sample II. And this happens in images taken with white light (compare figure 19 with figure 22): without the SIL it was not possible to see individual nanowires in Sample II, while they could be seen in Sample III; with the SIL on the other hand the nanowires are distinguished quite well in both samples, and maybe Sample II displays a slightly better contrast. As far as PL measurements are concerned, however, the difference is rather big. Despite the bigger pitch, the nanowire diameter was at the limit of resolution in Sample III, while nanowires could still be distinguished in Sample II. This is most probably where the substrate comes into play. As a matter of fact, Sample II consisted in rather longer nanowires, hence the substrate was further away from the emitting nanowires tops, and

moreover the nanowires themselves were more tightly distributed over the substrate, being the pitch smaller. On the other hand, in Sample III not only the nanowires were shorter, but aso less tightly distributed. This might have determined a higher influence from the substrate, which lowered the quality of the PL image.

5 Results and resolution evaluation

The previous section showed how the solid immersion technique could represent a valid tool for the optical characterization of patterned nanowires sample, as there seemed to be an actual improvement in resolution when the SIL was used. Thus, the objective of this chapter will be to introduce a theoretical model in order to actually quantify the improvement introduced by the SIL.

5.1 Experimental magnification factor

The SIL, being a lens, introduces its own magnification factor, that was estimated experimentally using the images taken from the samples described in section 4.1. Theoretically, the magnification factor introduced by the SIL should be equal to the refractive index n of the material which the SIL is made of. In this case the refractive index of LaSFN9 is equal to 1,816 at 587 nm. To obtain this factor experimentally one can just compare the size of the same object in images acquired with and without the SIL, in terms of number of pixels in the images. Then the magnification factor follows. This simple procedure was repeated on a few features of the sample pattern, to obtain an average value, and the magnification factor resulted to be equal to 1,9. This is quite consistent with the theoretical value if one takes into account also the oil layer between the sample and the solid immersion lens, which can alter the magnification factor to some extent in case there is a difference between the refraction indexes. In figure 27 two images of a plus sign in the pattern can be seen. The plus figure appears to have roughly the same size in the two pictures, because the image shown in figure 27a was taken with a 100x objective without the SIL, while the one in figure 27b was taken with a 50x objective with the SIL, but the SIL magnification factor of 1,9 roughly compensate for this difference.

5.2 Theoretical model for resolution evaluation

A generic optical system can be characterized by its response to a point light source (or a point object). This is the so called Point Spread Function (PSF), and its shape is linked to the resolution of the system. An optical system with high resolution will have a PSF that resembles an impulse function (i.e. there is signal just in perfect correspondence to the object), while an optical

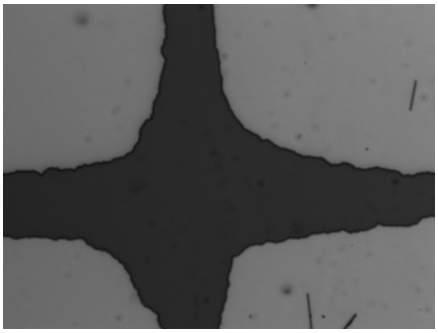

(a) Image taken without the SIL, with a 100x objective.

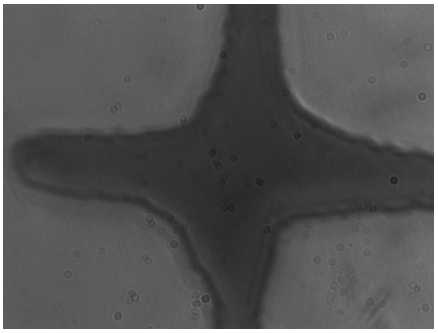

(b) Image taken with the SIL, with a 50x objective.

Figure 27: Images of the same pattern feature.

system with a low resolution will display a broad PSF. It is reasonable, even if it is not strictly exact, to consider the PSF of the system used the this thesis project as a gaussian, as it can be seen in figure 28. When an image of

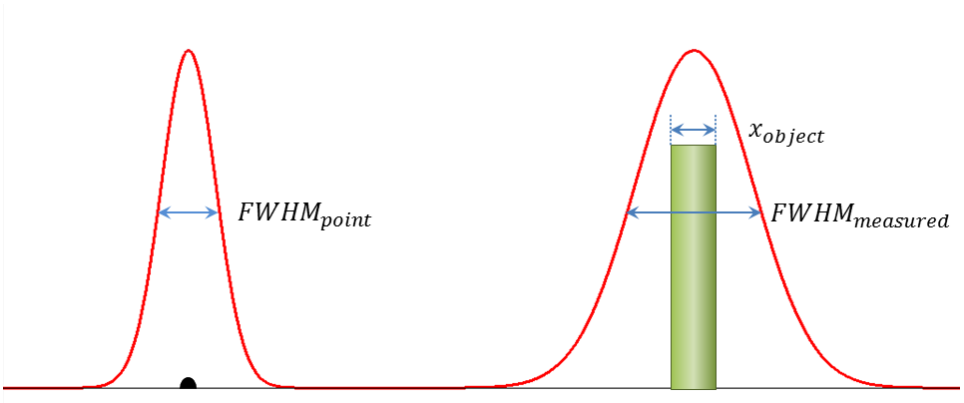

Figure 28: Point Spread Function of an optical system, and measured signal coming from an object.

an object which is not a point (but is still relatively small, e.g. a nanowire) is taken, the width of the object itself comes into play and the result will be a broader distribution, which can be considered to be gaussian as well and whose full width at half maximum ($FWHM_{measured}$) is linked to the PSF of the system by the relation:

$$FWHM^2_{measured} = FWHM^2_{point} + x^2_{object}. \tag{3}$$

This relation comes from the fact that the resulting intensity profile of a measurement is obtained by the convolution product of the PSF with the object. When a gaussian profile is convolved with another gaussian, the result is still a gaussian whose squared FWHM is the sum of the squared FWHMs of the starting gaussians, and the relation above is therefore valid, even if the object is not strictly a gaussian profile.
Knowing $FWHM_{measured}$ is important, as it represents how a single object is seen by the system, and it is the basis to develop a theoretical model of how an array of single objects is seen by the system. In order to get an experimental estimate of $FWHM_{measured}$, the samples described in section 4.1 were used. The size of the object in this case was known, since it was the thickness of the deposited nanowires. Measuring $FWHM_{measured}$, $FWHM_{point}$ could be derived from equation 3.
When two objects are close to each other, according to the Rayleigh criterion they can be resolved only if the distance between them is at least such that the principal maximum of one object (the only maximum if one takes a gaussian approximation) overlaps with the first minimum of the other. Beyond this distance the two objects are not resolved, as it can be seen in figure 29. When several objects are placed in an array with uniform spacing, theoreti-

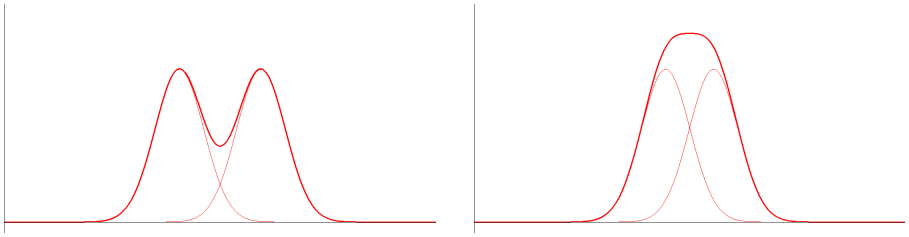

(a) Two objects at the limit of resolution according to Rayleigh criterion.

(b) Two objects beyond the limit of resolution according to Rayleigh criterion.

Figure 29

cally a gaussian signal with width $FWHM_{measured}$ will correspond to each object, so that the resulting signal from the array will be a periodic function, as shown in figure 30. The $FWHM_{array}$ of the periodical signal is no longer the one of the single objects, and the sum signal will also display a particular contrast value, which corresponds to how deep the dips between different peaks are and is calculated as the absolute difference between the peak and the valley values. If the distance between the objects forming the patten is

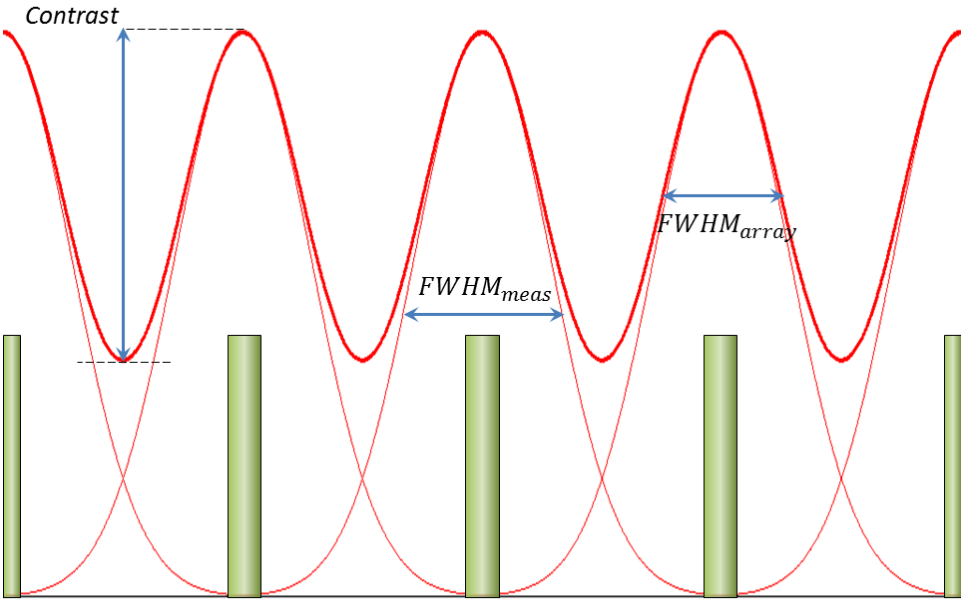

Figure 30: Theoretical signal generated by an array of objects.

fixed and known, both $FWHM_{array}$ and the contrast will be affected only by $FWHM_{measured}$, which is to say that they are indicators of the resolution. Unfortunately it is not possible to use just one of them to estimate the resolution of the system, as they both change when $FWHM_{measured}$ changes, according to the plots shown in figure 31. From the inspection of figure 31 it is possible to see that $FWHM_{array}$ present a sort of saturation behaviour, where the saturation value is half the spacing in the array. At this point, if $FWHM_{measured}$ grows larger only the contrast will get worse. In this region the objects cannot be considered as resolved according to the Rayleigh criterion. Thus, even if it is not possible to estimate directly the resolution from an array measurement, one can at least understand whether or not the objects are resolved according to the Rayleigh criterion, by looking at $FWHM_{array}$ and comparing it with the spacing between the array elements.

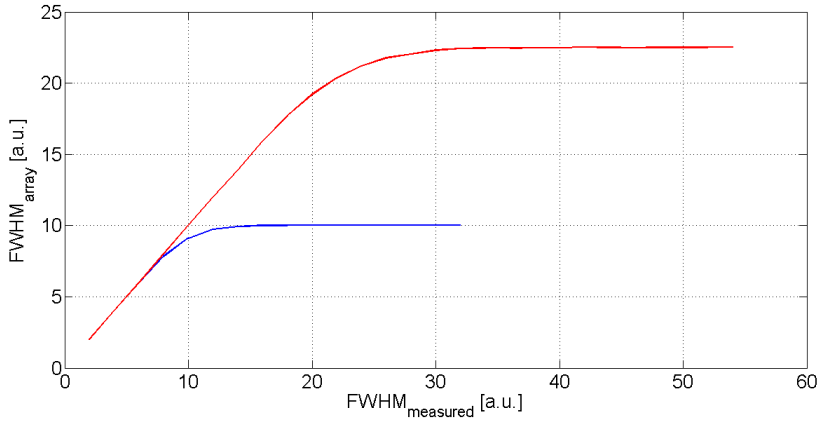

(a) Plot of $FWHM_{array}$ as a function of $FWHM_{measured}$ with distance 20 a.u. (blue curve) and 45 a.u. (red curve) between the objects in the array.

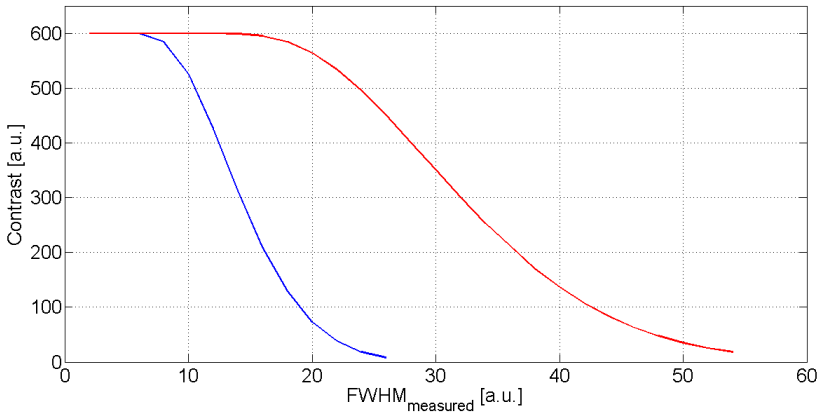

(b) Plot of the contrast as a function of $FWHM_{measured}$ with distance 20 a.u. (blue curve) and 45 a.u. (red curve) between the objects in the array.

Figure 31

5.3 Experimental resolution evaluation

In order to understand whether the SIL introduces a resolution improvement or not, and to quantify this improvement if possible, it is essential to establish a correlation between the dimensions of the images (expressed in terms of pixels) and the real distances between the features of an array (expressed in terms of nm). Considering the width of the CCD camera, the number of pixels, the magnification of the objective and the presence of a lens in front of the spectrometer, it has been evaluated that one pixel in an image taken without the SIL corresponds to approximately 89 nm. This was obtained by measuring the pitch of sample I, II and III in terms of pixel using intensity cutlines taken from the white light pictures, and comparing this values to the real pitch values (which were known from SEM measurements). The values obtained from the three samples were in good agreement. When the SIL is used, the magnification factor of 1,9 changes this value to 46,8 nm per pixel. This considered, it was possible to evaluate the PSF of the system both with and without the SIL, using the samples described in section 4.1. It was reasonable to assume that the thickness of the nanowires in the two samples was smaller (or at least comparable) with the width of the PSF of the system, $FWHM_{point}$. Then, referring to figure 28, it was possible to evaluate $FWHM_{measured}$ by taking intensity cutlines perpendicular to the nanowires and to derive $FWHM_{point}$ using equation 3. The results are shown in table 2.

Table 2

		Without SIL		**With SIL**	
	x_{obj}	Γ_{meas}	Γ_{point}	Γ_{meas}	Γ_{point}
Sample 1	80 nm	587,4 nm	582 nm	341,64 nm	332 nm
Sample 2	130 nm	649,7 nm	636 nm	373 nm	349 nm

As it can be seen from the values in the table, the SIL introduces a remarkable improvement in the PSF of the system. As a matter of fact, the nanowires appear to have roughly the same size (in terms of pixels) with or without the SIL (see figure 8a and 8b), where the nanowires with the SIL should have been larger by a factor 1,9 if the resolution was unchanged. This suggests that there is definitely an improvement in resolution due to the presence of

the SIL. Although the exact values of $FWHM_{point}$ are a bit different for the two different nanowires, one can conclude that the agreement between the value (especially as far as the SIL is concerned) is rather good and that $FWHM_{point}$ is around 600 nm without the SIL and around 320 nm with the SIL. Note these two values differ by a factor of roughly 1,9 which is to say that the SIL should improve the resolution by a factor of 1,9.
Now that $FWHM_{point}$ has been estimated, the data coming from the measurements can be fitted with a model coherently with what explained in section 5.2. This can be applied to the samples described in sections 4.4 and 4.5, as they proved themselves to be the most suitable ones to test the SIL, both in PL and reference light.
As far as the sample described in section 4.4 is concerned, a cutline was taken as shown in figure 32, both in the PL and reference light images. The inten-

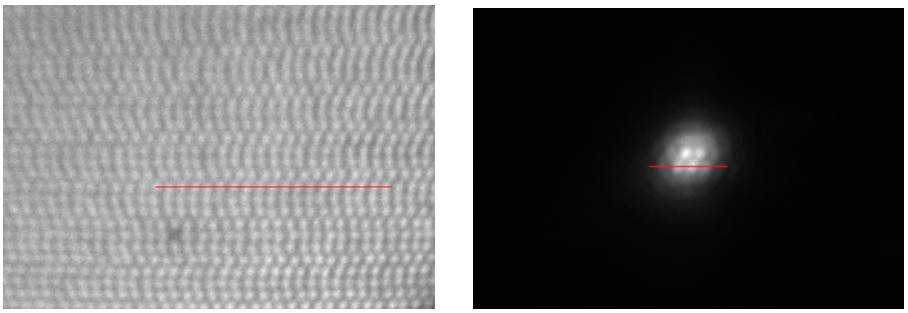

(a) Reference light image with cutline. (b) PL image with cutline.

Figure 32

sity profile taken from figure 32a is shown together with the model curves generated by each single nanowires and their sum, in figure 33. A constant value is also introduced into the model in order to consider the substrate. Figure 33 can be used to establish whether or not the nanowires in the picture are resolved. By inspecting the plot, one can see that the average value of $FWHM_{measured}$ is 327,6 nm, which is in very good agreement with what has been calculated for the deposited nanowires sample. The nanowires deposited on sample 2 had the same thickness as the ones standing in the array of this sample, and the single nanowire gaussian fitted by the model is coherent with the experimental gaussian obtained from single deposited nanowires in sample 2. Also $FWHM_{array}$ is worth to be considered, as it has an average value of 187,2 nm which is less then half the distance between

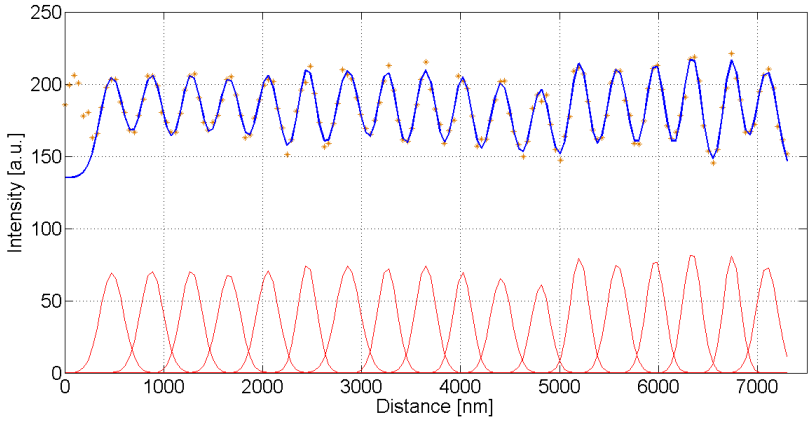

Figure 33: Intensity cutline from figure 32a: the orange dots are the experimental points; the blue curve is the model sum signal; the red gaussians are the model signals from single nanowires.

the nanowires. According to what was discussed in the previous section, and particularly referring to figure 31a, the nanowires can be considered as fully resolved here. The same method has been used to obtain the plot shown in figure 34 from the cutline of figure 32b. Considering what is shown in figure

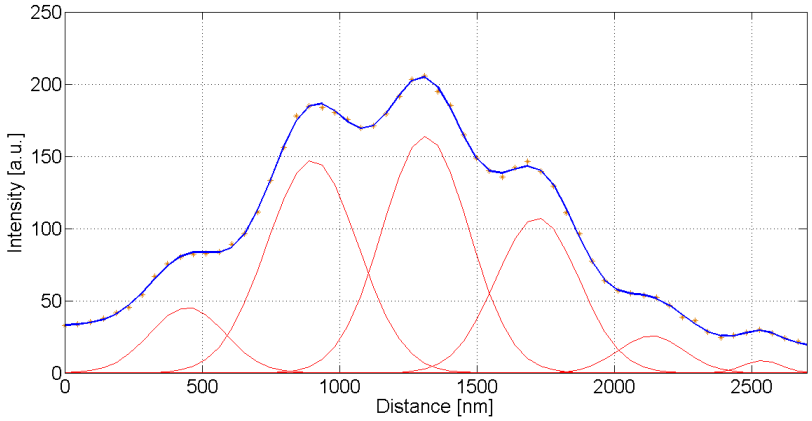

Figure 34: Intensity cutline from figure 32b: the orange dots are the experimental points; the blue curve is the model sum signal; the red gaussians are the model signals from single nanowires.

34, it can be verified that the theoretical $FWHM_{measured}$ is roughly the same for each nanowire and the average value is 312,15 nm, which is also in

good agreement with what has been found inspecting the reference light image. This suggests that the nanowires are resolved also in the PL image. On the other hand, the intensity with which the nanowires emit light is highly inhomogeneous, due to the fact that the excitation intensity itself (the laser beam intensity) varies with a gaussian profile. This unfortunately makes the model developed in the previous section unapplicable. Thus it is not possible to provide a quantitative evidence that the nanowires are resolved. To solve this problem, one should have a more homogeneous excitation source, so that all the nanowires in a certain area emit light with roughly the same intensity.
The images taken from the sample described in section 4.5 were unfortunately of lower quality, but still the improvement provided by the SIL is clear. Intensity cutlines were taken from the reference light images and they are shown in figure 35. The intensity profiles resulting from the cutline of

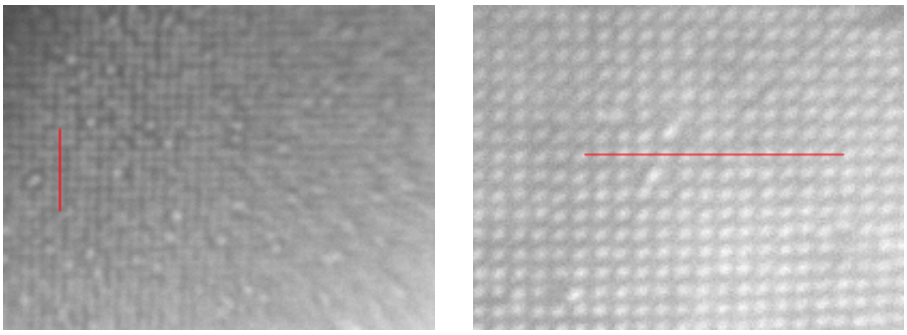

(a) Cutline taken from the image without SIL.

(b) Cutline taken from the image with SIL.

Figure 35

figures 35a and 35b are shown respectively in figures 36 and 37. It is clear that without the SIL the nanowires are below the limit of resolution, and some of them generate even one single broad peak with the neighbours. If one measures $FWHM_{array}$ in the picture taken without SIL, it results to have an average value very close to 250 nm, which is the half of the distance between the nanowires, and this is coherent with the model presented in the previous section. In presence of the SIL on the other hand, the model fits quite well to the measurements and an average $FWHM_{array}$ of 205,6 nm is obtained. This value grants that the nanowires are resolved and also the theoretical $FWHM_{measured}$ average value of 304 nm is consistent with the

measurements on single deposited nanowires and suggests that the thickness of the nanowires in this sample should be comparable to the one in the sample described in section 4.4.
The resolution in PL images was worse than in reference light images. In spite of the fact that the SIL allowed to get a glimpse of the presence of distinct nanowires whereas this wasn't possible wihtout the SIL, the improvement was not enough and the nanowires were below the resolution limit.

Intensity profile were examined also in the images taken from the LED

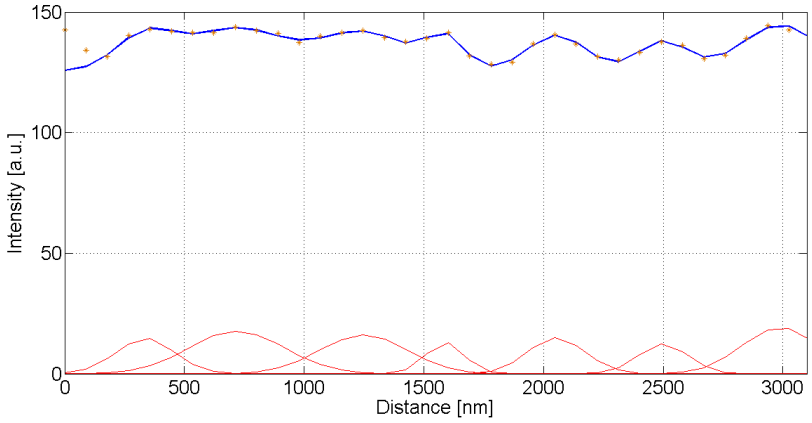

Figure 36: Intensity cutline from figure 35a: the orange dots are the experimental points; the blue curve is the model sum signal; the red gaussians are the model signals from single nanowires.

sample described in section 4.6. EL Images taken with and without the SIL are presented together with the cutlines in figure 38. It can be easily noted by inspecting figure 38 that the image taken with the SIL displays a lower contrast, hence the image taken without the SIL appears to have a higher quality. Nevertheless, it is worthwhile to examine the intensity profiles obtained from the cutlines. The intensity profile coming from the cutline in figure 38a is presented in figure 39. The average value of $FWHM_{measured}$ is 1,48 μm, while the average value of $FWHM_{array}$ is 1,13 μm, which is less than the half of the value of the pitch (which is known to be 2,5 μm). The nanowires are therefore fully resolved. In figure 40 on the other hand is shown the intensity profile from the cutline presented in figure 38b. From the inspection of figure 40 it can be found that the average of $FWHM_{measured}$ is equal to 1,09 μm, which would suggest that also in this case the narrower

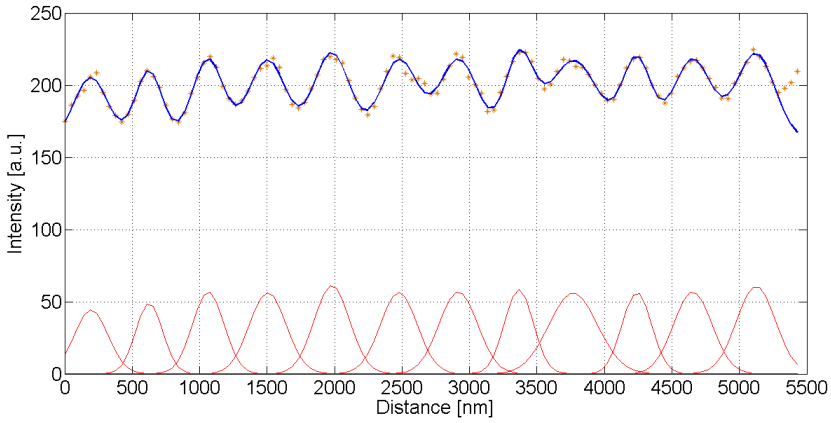

Figure 37: Intensity cutline from figure 35b: the orange dots are the experimental points; the blue curve is the model sum signal; the red gaussians are the model signals from single nanowires.

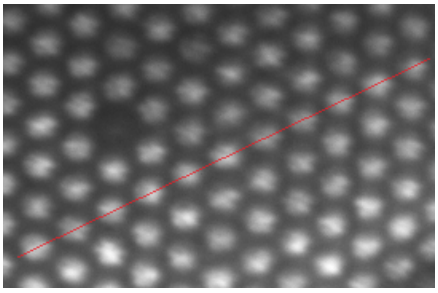

(a) Cutline taken from the image without SIL.

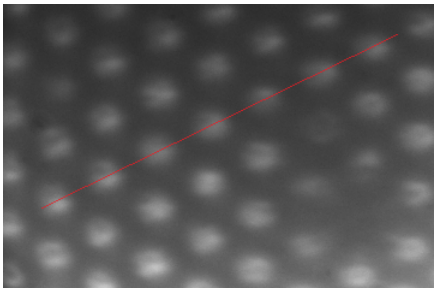

(b) Cutline taken from the image with SIL.

Figure 38

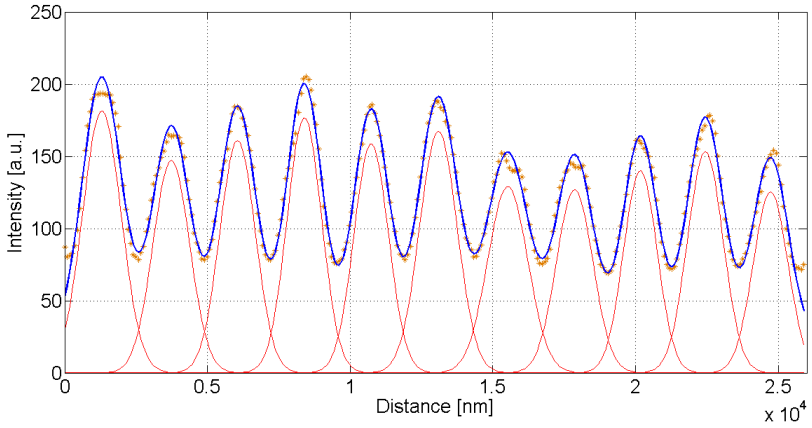

Figure 39: Intensity cutline from figure 38a: the orange dots are the experimental points; the blue curve is the model sum signal; the red gaussians are the model signals from single nanowires.

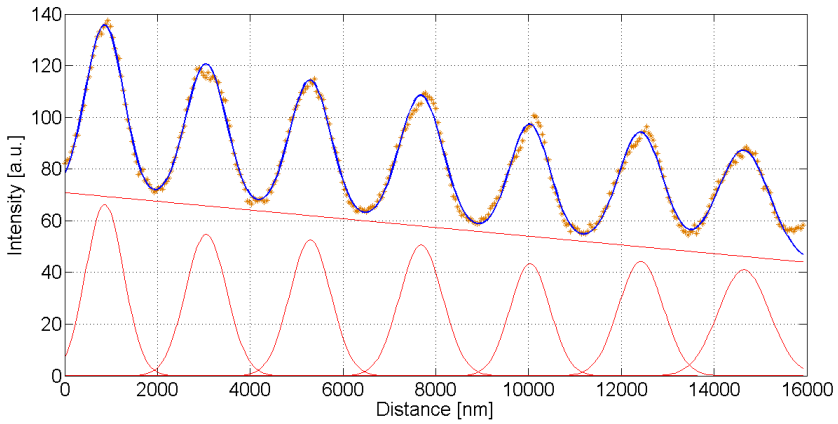

Figure 40: Intensity cutline from figure 38b: the orange dots are the experimental points; the blue curve is the model sum signal; the red gaussians are the model signals from single nanowires. The red line is counting for a linear background which is probably due to misalignment between the SIL stage and the sample stage or ti a tilt of the stage.

PSF of the system in the presence of the SIL might improve the resolution. Also the average value of $FWHM_{array}$ is lower than in the case without SIL and is equal to 1 μm, which is very close so $FWHM_{measured}$ and would hence indicate that the nanowires are even better resolved. Nevertheless, as discussed in section 5.2, it is difficult to evaluate the resolution because both contrast and $FWHM_{array}$ affect it. Hence, the fact that the images taken without the SIL display such a better contrast makes it hard to say whether or not there is an actual improvement by using the SIL in this particular measurements. Having a similar sample with a smaller pitch would reveal whether or not the contrast is more important than $FWHM_{array}$ when the goal is to resolve single objects in an array. All in all it was possible to disinguish between single nanowires both with and without the SIL and spectral measurements could be taken, so that the spectrum coming from each single nanowires could be actually analyzed. A line by line spectral scan taken from the LED sample without the SIL is shown in figure 41. Here the slit in the spectrometer was narrowed down until 0,1 mm so that a single line of nanowires could enter the image. The light recorded by the different line scans is consequently generated by a single nanowire.

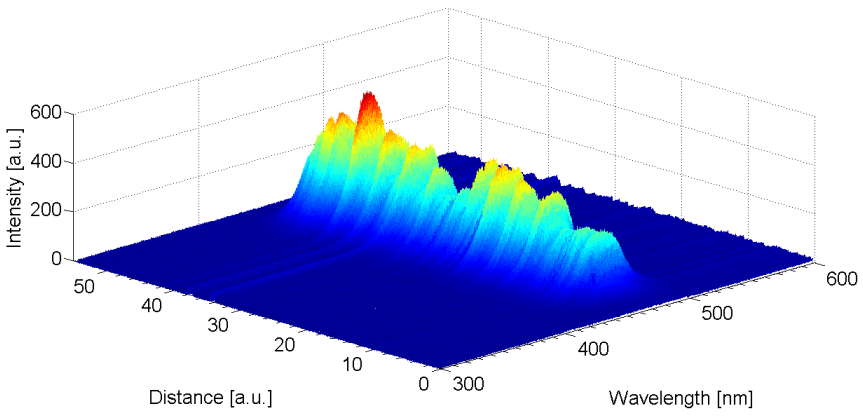

Figure 41: Line by line scan taken from a single nanowires line.

6 Conclusions and outlook

The goal of this thesis work was to explore the resolution limits of optical microscopy, and to establish if solid immersion microscopy can provide room for improvement particularly with the purpose of distinguishing single nanowires in nanowire array patterned samples. The goal can be considered as achieved as far as white light microscopy is concerned, since using the SIL brought improvements in almost all the sample that have been tested, and in most cases the improvement was supported by quantitative evidences. Photoluminescence measurements revealed themselves to be more laborious, as the excitation area was in most cases small and the excitation intensity was not uniform. Because of this, it was often difficult to evaluate the resolution in images taken with the SIL and providing quantitative evidences was more difficult. However, it was quite clear that solid immersion microscopy allowed a better resolution than normal optical microscopy. With a more uniform signal coming from the nanowires, distinction between single nanowires would have been possible even for arrays with pitches of a few hundreds of nanometers. Finally, electroluminescence measurements were performed on a sample with a relatively high pitch, which allowed also conventional optical microscopy to resolve single nanowires and collect light coming from each one of them. Nevertheless, also in this case the SIL provided a fairly good resolution, and more measurements can be performed to actually quantify the improvement in the resolution.

The continuing step of this project would be to test different materials in order to improve the collection efficiency of the technique. Ideally a higher collection efficiency would provide better quality images with a higher contrast. It can be interesting to test different immersion oils or even wax, to ascertain which one suits this technique better. On the other hand SIL made of different materials can be fabricated. A SIL with a higher refractive index should boost the resolution even more, but one should be careful in general about absorption problems that can rise especially when working with UV light. As far as the LED sample is concerned, another aspect that needs improvement is the stage which the sample is mounted on. During the project a rather stable stage was assembled but there were still some tilt problems as the inclination of the sample was difficult to control, and this might have caused intensity gradients in the images. An improved solid immersion microscopy would allow to observe and distinguish single nanowires in LED

devices with smaller pitch, both in white light images and spectrally, so that samples could be effectively characterized both spatially and based on their emission.

7 Acknowledgements

I would like to thank my supervisor Dan Hessman, for giving me the opportunity to work on this very interesting project.
My biggest thanks go to David Lindgren for his huge patience and willingness, for helping me with any experimental issue I had and for all the precious advices that he gave to me. I would also like to thank him for insisting on speaking swedish with me even in the beginning when the communication was not so efficient.
I would also like to thank all the people that made this work possible: prof. Anders Gustafsson who helped me fabricating the SIL; Kristian Storm, with whom I also had the pleasure to work; Zhaoxia Bi, Magnus Borgström, Daniel Jacobsson, Magnus Heurlin, Jesper Wallentin, and Gustav Nylund who provided me the samples together with all the information I needed. The company GLO for providing the LED sample.
Finally I would like to thank Golnaz Sherafatipour, David Göransson and Bita Malekian for all the chats and the company during these months of work.

References

[1] Wallentin et al. InP Nanowire Array Solar Cells Achieving 13.8% Efficiency by Exceeding the Ray Optics Limit. *Science* 1 March 2013: Vol. 339 no. 6123 pp. 1057-1060

[2] C Patrik T Svensson et al, Monolithic GaAs/InGaP nanowire light emitting diodes on silicon, 2008 *Nanotechnology* 19, 30.

[3] S. M. Mansfield and G. S. Kino. Solid immersion microscope. *Appl. Phys. Lett.* 57, 2615 (1990).

[4] S. M. Mansfield, W. R. Studenmund, G. S. Kino, and K. Osato. High-numerical-aperture lens system for optical storage *Opt. Lett.* 18,305 (1993).

[5] Masahiro Yoshita, Takeaki Sasaki, Motoyoshi Baba, and Hidefumi Akiyama. Application of solid immersion lens to high-spatial resolution photoluminescence imaging of GaAs quantum wells at low temperatures. *Appl. Phys. Lett.* 73, 635 (1998).

[6] Nikolay Panev, *Photoluminescence Studies of Single Quantum Dots*. PhD thesis, Lund University, 2004.

[7] Saleh, Teich (2007). Fundamental of Photonics. Wiley.

[8] Sang-Youp Yim, Joon Heon Kim, and Jongmin Lee. Solid Immersion Lens Microscope for Spectroscopy of Nanostructure Materials. *Journal of the Optical Society of Korea* Vol. 15, No. 1, March 2011, pp. 78-81

[9] Kazuko Koyama, Masahiro Yoshita, Motoyoshi Baba, Tohru Suemoto, and Hidefumi Akiyama. High collection efficiency in fluorescence microscopy with a solid immersion lens. *Appl. Phys. Lett.* 75, 1667 (1999)

[10] http://en.wikipedia.org/wiki/Airy_disk

[11] S. Moehl, Hui Zhao, B. Dal Don, S. Wachter, and H. Kalt. Solid immersion lens-enhanced nano- photoluminescence: Principle and applications. *J. Appl. Phys.* 93, 6265 (2003).

[12] http://refractiveindex.info/?group=SUMITA&material=KI-LaSFn9

[13] http://microscopy.zeiss.com/content/dam/Microscopy/Downloads/Pdf/MSDS/MSDS-Immersol-518F.pdf

Popular Science

Over the last decade the research in the nanotechnology field has improved significantly, and with the birth of the nanowires technology this branch of science could find countless new applications. A nanowire is a nanostructure with a diameter of the nanometer order of magnitude (often several tenths of nanometers) which can be fabricated in a lot of different ways, might they be top down processes such as lithography or bottom up processes such as crystal growth. Nanowires are particularly interesting because their really low dimensionality allow to create junctions between different materials that cannot be joined in bulky conditions. One of the most interesting applications is to optoelectronics, where one wants to develop devices that could convert light into electrical power (e.g. solar cells) or vice versa (e.g. LED devices). As far as these purposes are concerned, nanowire based devices could in principle achieve better performances than devices based on conventional bulk semiconductor technology. Since an optoelectronic device such as a LED is composed of a surface over which billions of nanowires are grown (often organized into patterns) the performance of the device is not affected by the performance of each single nanowire as much as by the average performance of the nanowires. Nevertheless, characterizing single nanowires in an array might be important, since in this way one can get insights that can be useful in order to improve the growth process for example. The average quality of the device is built by every single nanowire after all. Hence one might want to be able to detect the light coming from each separate nanowire, in order to analyze it and characterize it. There are already techniques that allow to get a "picture" of a nanowire sample with an extremely high resolution, such as the Scanning Electron Microscopy for example. But those "pictures" are not built upon the light coming from the object, as the conventional optical pictures are. Hence one might think to use optical microscopy if the goal is to detect and separate the light coming from the nanowires. The main issue is that the nano-features displayed by nanowires based devices are often below the resolution of conventional optical microscopy, which means that the nanowires cannot be distinguished if one looks at them with the usual microscope. Therefore one needs to find a way, if possible, to enhance the resolution of the optical microscopy technique, and this is what the project described in this article is about. A particular technique called Solid Immersion Microscopy was tested in order to see if it could provide a better

resolution than the conventional optical microscopy. The solid immersion microscopy employs a particular kind of lens, called Solid Immersion Lens (SIL). This lens works as illustrated in figure 42 and it is a hemispherical lens made of a high refractive index glass which is placed in direct contact with the sample. The SIL is supposed to improve the resolution of the optical system under a few different aspects. First of all, when light crosses the surface between two different optical media going from a lower refractive index medium to a higher refractive index medium (like in the case of a glass-air surface) a phenomenon called internal reflection becomes relevant and a big part of the light is reflected back into the high refractive index medium. The portion of light which is reflected increases with the angle of incidence, which means that a perpendicular angle of incidence will produce no reflection, and also with the difference between the refractive indexes involved. As it can

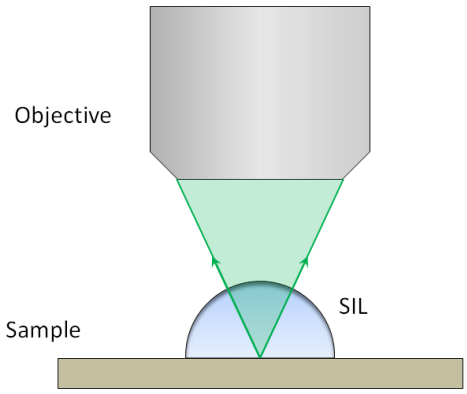

Figure 42: Schematic of the SIL experimental implementation.

be seen from figure 42, there are two main boundary surfaces at which internal reflection occurs: the one between the sample and the SIL, and the one between the SIL and the air. The SIL reduces the internal reflection in correspondence to the former, since its refractive index is intermediate between the one in the sample and the one in the air. Moreover, internal reflection is in principle completely got rid of correspondence of the latter boundary, and this is due to the geometry of the SIL which makes that the light encounters a perpendicular boundary surface at every angle. Basically it is as if the object and also the objective were immersed in a solid medium, since the light does not "sense" the glass-air boundary interface. Hence the name of the technique. The reduction of internal reflection also improves the

collection efficiency, which is the actual portion of the light emitted by the sample that can be collected by the objective. This is particularly important when the signal to be investigated is weak, and it might also contribute to provide an enhancement in the resolution.
In order to investigate if the improvements in resolution are significant, a SIL has been fabricated and tested on a number of different samples. Conventional white light images were taken from the samples first, where white light coming from a lamp was reflected by the sample. Subsequently attempts have been made to take also photoluminescence pictures and electroluminescence pictures. In both these cases the light is generated in the sample itself as a consequence of excitation processes of the electrons to higher energy states; light emission occurs when the electrons decay to lower energy states and the energy gap between the higher state and the lower state is released in the form of a photon. As far as photoluminescence (PL) is concerned, electron excitations are caused by the absorption of photons in the sample. Experimentally this is realized by shining a laser beam with a suitable energy onto the sample. On the other hand in electroluminescence (EL) the excitation process is due to an electrical current flowing through the sample. Experimentally this is realized by contacting the sample and connecting it to a voltage generator. Some examples are shown in figures 43, 44 and 45, as far as white light images and both PL and EL images are concerned. It is evident that the nanowires can be distinguished with the SIL whereas they could not without the SIL in white light and PL measurements. In the EL sample it was possible to distinguish them both with and without the SIL. As it can be seen in the figures the SIL allows often to distinguish

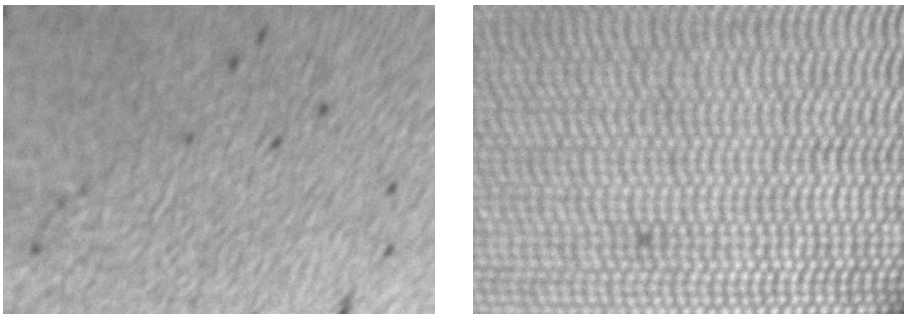

(a) Image taken without SIL.

(b) Image taken with SIL.

Figure 43: Examples of white light images from a nanowires sample.

(a) Image taken without SIL. (b) Image taken with SIL.

Figure 44: Examples of PL images taken from a nanowire sample.

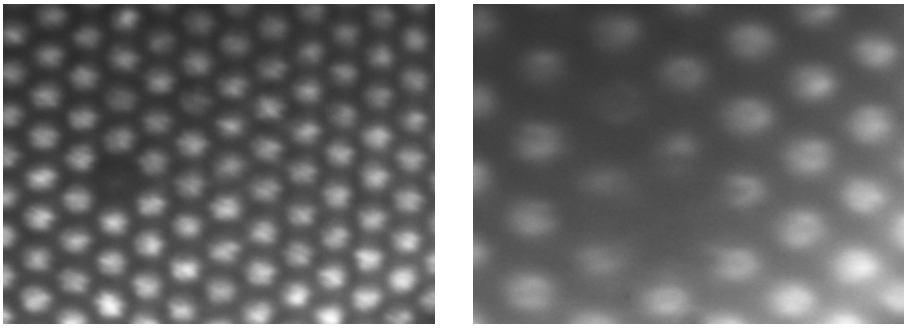

(a) Image taken without SIL. (b) Image taken with SIL.

Figure 45: Examples of EL images taken from a nanowire LED sample.

features that were impossible to observe with the conventional microscopy. Nevertheless the introduction of the SIL seems to lower the contrast of the images and hence the quality of the picture. To establish whether or not the resolution is enhanced, a theoretical model was created that took into account the presence of multiple objects (the nanowires) arranged in a periodical array. Intensity cut lines were then taken from the images and fitted to the theoretical model, in order to be able to evaluate the resolution of the system as far as a single object were concerned and more importantly to be able to make a comparison between optical microscopy and solid immersion microscopy. All in all, the SIL revealed itself to be a promising tool in order to enhance the resolution of optical microscopy. Further improvements are needed, but it appears that at least at some extent an enhancement in resolution is granted.